

Light force fluctuations in a strongly coupled atom-cavity system

T. Puppe, I. Schuster, P. Maunz,* K. Murr, P.W.H. Pinkse, and G. Rempe
Max-Planck-Institut für Quantenoptik, Hans-Kopfermann-Str. 1, 85748 Garching, Germany
(Dated: July 9, 2018, PREPRINT)

Between mirrors, the density of electromagnetic modes differs from the one in free space. This changes the radiation properties of an atom as well as the light forces acting on an atom. It has profound consequences in the strong-coupling regime of cavity quantum electrodynamics. For a single atom trapped inside the cavity, we investigate the atom-cavity system by scanning the frequency of a probe laser for various atom-cavity detunings. The avoided crossing between atom and cavity resonance is visible in the transmission of the cavity. It is also visible in the loss rate of the atom from the intracavity dipole trap. On the normal-mode resonances, the dominant contribution to the loss rate originates from dipole-force fluctuations which are dramatically enhanced in the cavity. This conclusion is supported by Monte-Carlo simulations.

INTRODUCTION

“As a subject of continuing interest light stands the test of time very well”, Knight and Allen wrote in 1983 [1]. Today, this is as true a statement as it was 24 years ago. There is hardly a laboratory without a laser and the quantum properties of light continue to rouse researchers’ interest. The ideal environment to study the interaction between light and matter at the level of single quanta is an optical cavity. In the strong-coupling regime, the periodic exchange of the excitation between the atom and the cavity is faster than all loss rates in the system, and the atom and cavity resonances exhibit an avoided crossing, as predicted by the Jaynes-Cummings model (JCM) [2, 3]. The resulting splitting, which exists in the limit of weak driving, is referred to as the “vacuum-Rabi” splitting. Indeed, the vacuum-Rabi splitting has become a benchmark measurement for strong coupling[4, 5].

Because of the coupling, the bare states of the atom and the cavity mode mix to form new energy eigenstates, the so-called “dressed states”. In a typical experiment the normal-mode splitting is measured in the excitation spectrum of the cavity. Since the transmission of the cavity is directly proportional to the cavity excitation, such a measurement is straightforward. From a theoretical point of view, measuring the atomic excitation via spontaneous emission is equivalent. The combination of these two measurements would complete the information on the excitation of the dressed-state constituents. Experimentally, however, the spontaneously emitted photons are not easily accessible. Recognizing that the recoils of spontaneous emission lead to heating of the atom, a naive picture predicts that the atomic excitation can be observed by monitoring the heating of an atom as a function of the laser frequency.

The normal-mode spectrum has been measured in both the transmission of the cavity and the loss rate of the atom from an intracavity trap [4]. It turns out that the loss spectrum cannot be explained by the spontaneous emission alone. This shows that the naive picture is incomplete because there are more light forces acting on an atom in a cavity than the one due to spontaneous emission. For instance, in addition to the (conservative) dipole force, theory predicts velocity-dependent light forces in a cavity, which are exploited in cavity cooling [6, 7, 8, 9]. The cavity is indispensable in this scheme, as it provides a necessary delay in the response of the field to the presence of the atom. The cavity also modifies the *fluctuations* of the light force, which increase the kinetic energy of an atom and thus open up an additional escape mechanism for an atom trapped inside the cavity. The rate at which the kinetic energy is increased is quantified by the momentum diffusion coefficient. Previous calculations [8, 10, 11, 12, 13, 14] have shown that dipole-force fluctuations can dramatically enhance momentum diffusion inside a cavity. A recent general derivation identifies a term in the diffusion coefficient which originates from the cavity dissipation[15]. Compared to the corresponding free-space situation, this leads to a large increase of the momentum diffusion.

The present paper gives a detailed account of the role of spontaneous emission and of the dipole-force fluctuations in a cavity QED system with single trapped atoms. Experimental data [4] are compared with Monte-Carlo simulations in which the different contributions to the light force can be evaluated individually. After a short introduction of relevant theoretical aspects of the atom-cavity system we show the experimental results and compare the data with detailed numerical simulations.

VACUUM-RABI SPLITTING

The closed quantum system composed of a single atom and a single mode of the light field was described by Jaynes and Cummings [2] and can be solved analytically. The Hamiltonian of a single mode of frequency ω_{cav} with creation

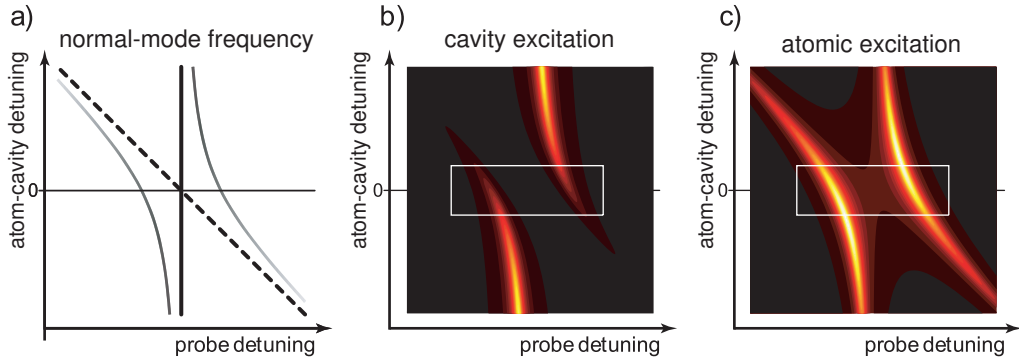


FIG. 1: Normal modes as a function of atom-cavity and (probe) laser-cavity detunings. a) The coupling of the atom (frequency determined by the straight dashed line) and the cavity (vertical solid line) generates two new eigenstates which are superpositions of atomic and cavity states (curved lines). For vanishing detuning between atom and cavity the dressed states reach the minimum separation of $2g$, the vacuum-Rabi splitting. b) Cavity excitation as a function of atom-cavity and probe detunings. c) Atomic excitation as a function of atom-cavity and probe detunings. The cavity excitation on the dressed-state resonances depends more strongly on the mixing angle than the atomic excitation, as only the cavity part of the dressed state is excited by the probe laser. In b) and c) the frequency range covered by the experiment (see Fig. 2) is indicated by the white rectangle.

operator a^\dagger in interaction with a two-state atom of frequency ω_{at} with lowering operator $\sigma = |g\rangle\langle e|$ in the dipole and rotating-wave approximation reads:

$$H_{JC}/\hbar = \omega_{cav}a^\dagger a + \omega_{at}\sigma^\dagger\sigma + g(a\sigma^\dagger + a^\dagger\sigma), \quad (1)$$

where g is the atom-cavity coupling constant. The two eigenstates $|+\rangle$ and $|-\rangle$ of the first excited doublet of the combined atom-cavity system are superpositions of the atomic ground state with one intracavity photon $|g, 1\rangle$ and the atomic excited state with zero photons $|e, 0\rangle$:

$$|+\rangle = \sin \theta |g, 1\rangle + \cos \theta |e, 0\rangle \quad (2)$$

$$|-\rangle = \cos \theta |g, 1\rangle - \sin \theta |e, 0\rangle. \quad (3)$$

These ‘‘dressed states’’ are obtained by a rotation in Hilbert space from the bare state basis $\{|g\rangle, |e\rangle\}$ to the dressed state basis $\{|+\rangle, |-\rangle\}$ by the mixing angle θ . The mixing angle ($0 \leq \theta < \pi/2$) is defined by $\tan 2\theta = -2g/\Delta$. It depends on the detuning between the cavity and the atomic resonance, $\Delta = \omega_{cav} - \omega_{at}$. For the detunings $\Delta = (-\infty, 0, \infty)$ the mixing angle is $(0, \pi/4, \pi/2)$. By convention [16], the energy of the state $|+\rangle$ is larger than that of the state $|-\rangle$. In the closed system, the dressed states have well-defined eigenenergies.

The open quantum system is subject to loss of photons from the cavity and spontaneously emitted photons from the atom and can be solved analytically in the limit of weak atomic excitation [10, 17]. To replenish lost photons, the system must be pumped by an incident light field, called probe laser. Since in our case only the cavity mode is excited by the probe laser, the excitation of a dressed state is proportional to the contribution of the cavity state to the dressed state and to the probe laser power. In the open quantum system the dressed states have finite energy uncertainties and, hence, finite linewidths. The excited bare cavity state and the excited atomic state have linewidths of 2κ and 2γ , respectively. In general, the linewidth of the dressed states will be given by a weighted average of 2κ and 2γ determined by the mixing angle. For large detunings the mixing angle is small such that the dressed states converge to the bare states with the corresponding linewidth.

Figure 1 b) shows the calculated cavity transmission as a function of the probe detuning and of the atom-cavity detuning. The probe detuning is indicated with respect to the cavity resonance. The transmission of the cavity is proportional to the number of photons in the cavity. Therefore the height of the two normal modes in the transmission spectrum is proportional to $\sin^2 \theta$ and $\cos^2 \theta$, respectively. For zero detuning between atom and cavity, the mixing angle is $\pi/4$ and the transmission at both normal-mode frequencies is equal. In this case, the distance between the two normal-mode frequencies reaches its minimum value of $2g$, the vacuum-Rabi splitting.

In contrast to the transmission, the calculated atomic excitation spectrum (figure 1 c) shows a different dependency of the peak height on the mixing angle. As here again the cavity is excited whereas now the atomic excitation is plotted, the height of both normal modes is proportional to $\sin \theta \cos \theta$ and hence only exhibits a weak dependency on the atom-cavity detuning.

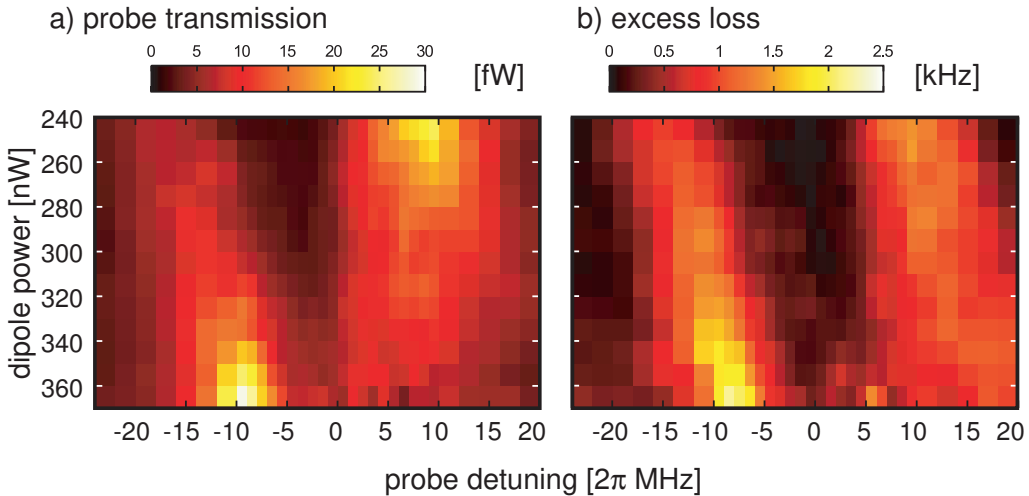


FIG. 2: Experimentally measured cavity transmission a) and excess loss rate b) as a function of dipole power and probe detuning. Tuning the dipole power changes the Stark shift induced by the trapping field and results in a change of the effective atom-cavity detuning. The two normal modes are clearly visible in the transmission. They show the expected dependence on the detunings. Compared to the transmission measurement, the observed excess loss rate has a weaker dependence on the atom-cavity detuning. In both a) and b) the broadening of the right normal mode with respect to the left one is a consequence of the atomic motion, as explained in the text. The data shown in figure 3 are also included in b).

THE EXPERIMENT

Our experimental setup and the measurement procedure used to observe the normal modes of a single atom strongly coupled to a cavity were described in detail elsewhere [4]. In short, laser-cooled ^{85}Rb atoms are injected into a high-finesse cavity with velocities below 10 cm/s. The cavity has a finesse of 4.4×10^5 , a mode waist of 29 μm and a length of 122 μm . It is near resonant with the $5^2S_{1/2}F = 3, m_F = 3 \leftrightarrow 5^2P_{3/2}F = 4, m_F = 4$ transition of ^{85}Rb at 780.2 nm. The maximum coupling constant for this transition is $g = 2\pi \times 16$ MHz. A weak red-detuned (785 nm) intracavity dipole field guides the atom into its antinodes. The dipole mode has two nodes fewer than the cavity-QED probe mode, so that the antinodes of the two modes coincide midway between the cavity mirrors. For the probe laser on resonance with the cavity, the presence of an atom leads to a distinct drop of the cavity transmission. When the transmission drops below a preset threshold, an atom must have entered a region where the antinodes of the trapping and probe fields overlap. The power of the dipole field is suddenly increased, trapping the strongly coupled atom with close to 100% efficiency. The dipole trap induces a position-dependent differential Stark shift between the ground and excited states of the atom, so that the detuning of the probe laser with respect to the atom becomes a function of the dipole laser power and of the position. After trapping the atom, the probe frequency and power is adjusted to perform the desired spectroscopy. For probe frequencies close to the normal modes, the dissipative light forces are strongly heating. These frequencies cannot be avoided when scanning across the spectrum. Therefore, measurement windows of 0.1 ms duration were interwoven with 0.5 ms long time windows in which the detunings are set for optimal cavity cooling [6], relocalizing the atom in the axial direction and obtaining information on the atom-cavity coupling for further data processing.

In figure 2 a), the cavity transmission is plotted as a function of the probe detuning for different trap depths given by the dipole laser power as measured in transmission. Only observation windows were used where the neighbouring cooling intervals indicated that the atom was well localized, “qualifying” those time windows where the atom was strongly coupled. For each setting of the dipole power, i.e., a horizontal line in the figure, two distinct resonances are observed when the probe detuning is scanned. As can be seen, the positions of the peaks vary with the dipole power. For small dipole power, the bare atomic resonance has a lower frequency than that of the cavity, and the asymmetric normal-mode spectrum shows the weak atom-like peak for negative probe detunings and a stronger cavity-like peak for small positive detuning of the probe light. For high dipole power, the effective atomic resonance is found at frequencies higher than the bare cavity resonance. The cavity-like peak, which is now the one at lower probe detuning, is again stronger. Hence, the data show the avoided crossing of the dressed states and the strong dependence of the transmission on the atom-cavity detuning is clearly visible.

In contrast to the cavity transmission, the atomic excitation cannot be measured directly in our experiment. We

can, however, experimentally determine the loss rate from the trap. From the observed mean storage time the *excess* loss rate is derived, defined as the surplus loss rate induced by probing the system. It is shown in figure 2 b). The simulations in the next paragraph show that the excess loss rate on the normal-mode resonances is dominated by heating generated by fluctuations of the dipole force. As will be discussed, it is actually because of the large enhancement of the dipole fluctuations in a cavity QED environment that the normal modes are clearly visible in the excess loss rate.

SIMULATIONS

To understand the details of the observed transmission spectra, in principle only the distribution function of the atomic position is required to determine the measured line shapes. The spatial distribution is governed by light forces, which can be calculated: our experiment operates at low saturation, where the atomic excitation is small ($P_e \approx |\langle \sigma \rangle|^2 \ll 1$). Here, analytical expressions for the expectation values of the dipole force, the velocity-dependent force and the momentum diffusion coefficient are available, even in the presence of the dipole trap, which gives rise to nontrivial changes of the light forces. One might therefore expect that the position distribution function can be predicted in a straightforward manner. This is not the case. The expressions for the forces depend strongly on the position of the atom and the light forces therefore determine the atomic motion in a very complex way. Moreover, the loss spectra depend even stronger on the details of the motion, and a position distribution function will not be sufficient to accurately predict the escape probability of an atom from the trap. This is the reason why we performed a Monte Carlo simulation and calculated many trajectories of single (point-like) atoms in three dimensions by integrating the Langevin equations of motion. The trajectory is determined by the frequencies of the atom, cavity and laser and the intensities of the standing-wave trapping and probe fields and their geometry. In order to model the experiment in detail, a single atom is injected transversally into the cavity from below. In the centre of the cavity the antinodes of the guiding and probe fields coincide. As in the experiment, the atom is thus guided into a region of strong coupling. For the parameters of the experiment, the presence of an atom leads to a distinct drop of the cavity transmission. When the simulated transmission drops below a threshold, the power of the intracavity dipole laser is increased to capture the atom. After trapping the atom, the sequential probing and cooling intervals are precisely simulated according to the experimental procedure.

Fluctuations of the dipole force increase the width of the momentum distribution. This is quantified by the momentum diffusion coefficient $2D = \frac{d}{dt} (\langle \mathbf{p}^2 \rangle - \langle \mathbf{p} \rangle^2)$. The expectation value of this diffusion coefficient can be calculated analytically in the regime of low saturation and in lowest order of the atomic velocity. The result can be expressed as the sum of a spontaneous emission term and a dipole force fluctuation term:

$$D = D_{\text{sp}} + D_{\text{dp}}. \quad (4)$$

The spontaneous emission term is directly proportional to the excitation of the atom, P_e :

$$D_{\text{sp}} = (\hbar k)^2 \gamma P_e. \quad (5)$$

As shown in Ref. [15], the dipole fluctuation term, D_{dp} , can be separated into two distinct contributions:

$$D_{\text{dp}} = |\hbar \nabla \langle \sigma \rangle|^2 \gamma + |\hbar \nabla \langle a \rangle|^2 \kappa, \quad (6)$$

where the mean coherence $\langle \sigma \rangle$ is to be evaluated within the cavity setting and $\langle a \rangle$ is the mean amplitude of the cavity field. The first term in D_{dp} can be interpreted as caused by a fluctuating atomic dipole coupled to a non-fluctuating light field. The second term in D_{dp} can be interpreted as caused by a fluctuating cavity field coupled to a non-fluctuating atomic dipole. The expression for D , Eqs. (4,5,6), is valid regardless of the value of the coupling g , the only condition is low saturation such that the internal state of the atom can be treated as a harmonic oscillator.

The two contributions to D differ in their spatial properties, which requires some care in the implementation into the simulation. The momentum diffusion due to the fluctuation of the dipole force is proportional to the square of the gradient of the atom-cavity coupling strength, which is about 50 times larger in axial direction than in the radial direction. Thus, the resulting heating is mainly directed along the cavity axis. In the simulation, the axial momentum of the atom is changed in each time step, the sign of the change chosen randomly with equal probability. The emission of a photon from the atom imprints the photon recoil of $\delta p = \hbar k$ on the motion of the atom. The spatial distribution of scattered photons and thus also of photon recoils is given by the emission characteristics of the polarized excited state of the atom. For ^{85}Rb atoms in the $F = 3, m_F = 3$ electronic ground state, which are excited

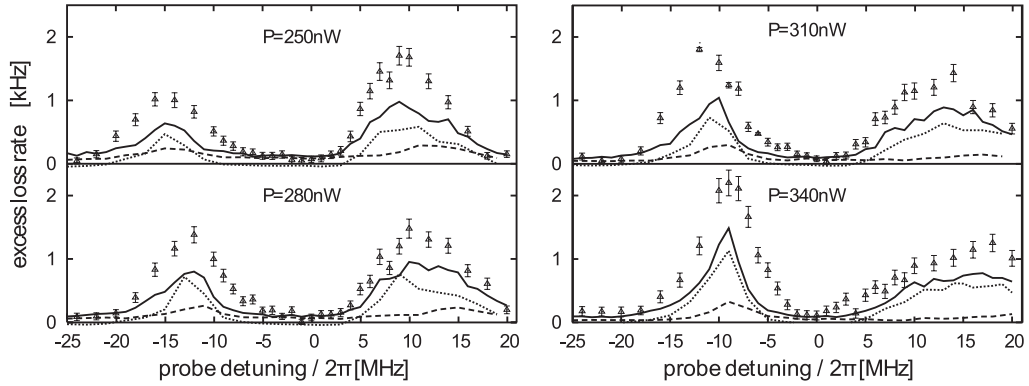


FIG. 3: Observed excess-loss rate of trapped atoms as a function of the probe detuning (triangles). On average each point includes the data from between 35 and 1000 atoms. The lines show results of the Monte Carlo simulation including spontaneous emission only (dashed lines), dipole fluctuations only (dotted lines), and the contribution of both heating mechanisms (solid lines).

by circularly polarized light, $2/5$ of the momentum diffusion acts in direction of the cavity axis, which coincides with the quantization axis, and $3/10$ points along each of the two orthogonal radial directions. This diffusion mechanism is included in the simulation by applying random momentum kicks. The momentum kicks which are used to generate the stochastic force reproduce the first moment of the spreading of the momentum distribution, the diffusion coefficient. For the numerical integration of the equations of motion a Runge-Kutta algorithm with adjustable step size is used. For stochastic processes, a highly uniform pseudorandom number generator is used, the “Mersenne Twister” [18].

In the experiment, the storage time in the trap without probe light is found to be limited by parametric heating. This heating is caused by technical fluctuations of the frequency difference between the trapping laser and the cavity resonance, resulting in intensity fluctuations of the intracavity field. A theoretical investigation [19] shows that the heating rate is proportional to the spectral noise power density of the intracavity intensity at twice the trap frequency. In the simulation, this heating mechanism is modelled by randomly changing the intensity of the trapping field in each time step δt . This leads to a white spectrum of the noise power density for frequencies up to $1/2\delta t$. The intensity in each time step is chosen according to a Gaussian distribution with mean value equal to the average intensity. The width of the distribution is adjusted to reproduce the experimentally observed storage time of an atom in the dark trap, without probe light. It is verified that for these fixed parameters, the model reproduces the observed storage times for different probe powers [6].

LIGHT-FORCE FLUCTUATIONS IN SIMULATION AND EXPERIMENT

Results of the simulation for the transmission of the cavity were shown in Ref. [4]. They agreed well with the experimental data if the power of the dipole laser was reduced by about 30% with respect to the intracavity power estimated from the measured cavity transmission. This could be explained by different transmission coefficients of the two cavity mirrors, which would lead to an error in the calibration of the intracavity light intensity. For consistency, the power of the probe light in the simulation is reduced by the same amount.

Results of the simulation for the excess loss are shown in figure 3, together with the data [4]. The loss spectra also show two well-resolved peaks at the normal-mode resonances. The left peak is observed to be narrower than the right peak. This is explained by the position-dependent Stark shift: if an atom oscillates in its dipole trap, it will experience different coupling strengths and different Stark shifts. Our trapping method ensures that atoms are stored in an antinode of the dipole trap overlapping with the antinodes of the cavity-QED field. Therefore, an atom closer to the centre of its local trap will experience a larger Stark shift and will simultaneously be stronger coupled. A stronger coupling will make the splitting between the normal modes larger; a stronger Stark shift will shift the entire spectrum to the right (towards larger probe detunings). Hence, for the left peak these two effects are opposed, while for the right peak they add up, which explains the fact that the left one is narrower than the right one. The results of the simulation reproduce this effect and predict the line shapes in the loss spectrum well. The residual differences in amplitude are considered small in view of the fact that absolute loss rates are calculated without free parameters.

We now analyse the role of the light forces and their contribution to the features in the spectrum. In this respect it is important to realize that cavity cooling (either during probing or during the cooling intervals) only cools the axial

motion in our setup. Hence, an atom is most likely to escape in radial direction after it is heated up by spontaneous emission recoils. The heating due to fluctuations in the amplitude of the dipole trapping field is strongest in the axial direction, where the gradients of the fields are largest. The heating in this direction is compensated by cavity cooling, also working in the axial direction. This leads to the hypothesis that the normal modes show up in the loss spectra because on the normal-mode resonances the excitation is large and spontaneous emission will heat up the atom in the transverse direction, where it will finally escape the trap. In the following we will see that this hypothesis is wrong.

In order to test our hypothesis, we exploit the possibilities of the simulation. In the simulation one has complete information about the atomic trajectory. This allows for example to test the role of the transverse heating due to D_{sp} by identifying the direction in which an atom escaped. Another advantage of the simulation is that it is possible to enable or disable individual light forces in a particular simulation run, and in this way determine the contributions of the individual forces. In figure 3 simulated loss spectra considering only heating from spontaneous emission ($D_{sp} > 0, D_{dp} = 0$) are compared with simulations taking into account fluctuations of the dipole force only ($D_{sp} = 0, D_{dp} > 0$) and a simulation including both diffusion mechanisms ($D_{sp} > 0, D_{dp} > 0$). As expected, the results with only the spontaneous emission heating (dashed line) show a normal-mode spectrum. However, in addition to the difference in overall amplitude, also the shape of the simulated spectra differs from the measured loss spectrum. This falsifies the above hypothesis and one is forced to conclude that other heating mechanisms must play an important role.

The results of the simulation with only the dipole fluctuations enabled (dotted line) show a normal-mode spectrum, which fits the data better than the simulation with only the spontaneous emission enabled. This result hints that on the normal-mode peaks the axial heating is compensated insufficiently. The particle can then escape in axial direction. This can be investigated in the simulation with all forces (solid line), which describes the data best. The results show that for zero and large probe detunings, spontaneous emission dominates the losses. Here an atom leaves the cavity with high probability in the transverse direction, the direction in which heating is not compensated by cooling. If the probe light is resonant with one of the normal modes, momentum diffusion induced by dipole fluctuations dominates and causes more than two thirds of the loss rate. In the simulation it is indeed observed that on the normal-mode peaks, a significant amount of the atoms escape in the axial direction. The conclusion is that on the normal modes, the larger momentum diffusion is only partly compensated by cavity cooling in the neighbouring cooling intervals.

The data show that the cavity-enhanced momentum diffusion is a real and important process that cannot be neglected in experiments with high-finesse cavities. It should be emphasized that this finding is in accordance with theory: momentum diffusion on the symmetric normal-mode resonances for an atom in our cavity is about 50 times larger than in free space for the same intensity of a standing wave probe field [20]. Between the normal-mode resonances, the contribution of this term is close to zero; for probe frequencies far detuned from the normal modes, the term falls off quadratically. It is this remarkably large enhancement of D_{dp} at the normal modes which makes the normal modes clearly visible in the excess loss rate.

CONCLUSION

In conclusion, we have observed the avoided crossing between the dressed states of a strongly coupled atom-cavity system. The crossing is clearly visible in both the transmission and in the loss rate. Comparison of the latter with simulations allows to deduce the relative importance of different heating mechanisms and gives evidence for strong cavity-enhanced heating on the normal-mode resonances, an effect which permits the clear observation of the normal modes in the loss rate in the first place. It should be emphasized that on the normal-mode resonances the dominating heating originates not only from the enhanced atomic dipole fluctuations, but also from enhanced fluctuations of the cavity field, which significantly exceed the fluctuations in free-space fields for the same intensity.

* present address: FOCUS Center and Department of Physics, University of Michigan, Ann Arbor, Michigan 48109, USA

[1] P.L. Knight and L. Allen, *Concepts of Quantum Optics*, Pergamon, Oxford 1983.

[2] E.T. Jaynes and F.W. Cummings, Proc. IEEE **51** 89 (1963).

[3] B.W. Shore and P.L. Knight, J. Mod. Opt. **40** 1195 (1993).

[4] P. Maunz, T. Puppe, I. Schuster, N. Syassen, P.W.H. Pinkse, and G. Rempe, Phys. Rev. Lett. **94** 033002 (2005).

[5] A. Boca, R. Miller, K.M. Birnbaum, A.D. Boozer, J. McKeever, and H.J. Kimble, Phys. Rev. Lett. **93** 233603 (2004).

[6] P. Maunz, T. Puppe, I. Schuster, N. Syassen, P.W.H. Pinkse, and G. Rempe, Nature **428** 50 (2004).

[7] T.W. Mossberg, M. Lewenstein, and D.J. Gauthier, Phys. Rev. Lett. **67**, 1723 (1991)

- [8] P. Horak, G. Hechenblaikner, K.M. Gheri, H. Stecher, and H. Ritsch, Phys. Rev. Lett. **79** 4974 (1997).
- [9] V. Vuletic and S. Chu, Phys. Rev. Lett. **84**, 3787 (2000).
- [10] G. Hechenblaikner, M. Gangl, P. Horak, and H. Ritsch, Phys. Rev. A **58** 3030 (1998).
- [11] T. Fischer, P. Maunz, T. Puppe, P.W.H. Pinkse, and G. Rempe, New. J. Phys. **3**, 11.1 (2001)
- [12] K. Murr, J. Phys. B **36** 2515 (2003).
- [13] P. Domokos, P. Horak, and H. Ritsch, J. Phys. B: At. Mol. Opt. Phys. **34** 187 (2001).
- [14] P. Domokos and H. Ritsch, J. Opt. Soc. Am. B **20** 1098 (2003).
- [15] K. Murr, P. Maunz, P.W.H. Pinkse, T. Puppe, I. Schuster, D. Vitali, and G. Rempe, Phys. Rev. A **74** 043412 (2006).
- [16] C. Cohen-Tannoudji, J. Dupont-Roc, and G. Grynberg, *Atom-Photon Interactions: Basic Processes and Applications*, Wiley and Sons, New York 1992.
- [17] H.J. Carmichael, *An Open Systems Approach to Quantum Optics*, (Springer-Verlag Berlin, 1991).
- [18] M. Matsumoto and T. Nishimura, ACM Trans. Model. Comput. Simul. **8** 3 (1998).
- [19] T.A. Savard, K.M. O'Hara, and J.E. Thomas, Phys. Rev. A **56** R1095 (1997).
- [20] The cavity enhancement of the momentum diffusion [8, 10, 11, 12] on the symmetric normal-mode resonances reduces to $8C/(1 + \gamma/\kappa)$. With the cooperativity $C = g_{\text{eff}}^2/(2\gamma\kappa)$ and an effective coupling strength of $g_{\text{eff}} = 13 \times 2\pi$ MHz obtained from the simulations, we find an enhancement of 51.